

Combinatorial Approach to Thin-Film Silicon Materials and Devices

Preprint

Q. Wang, H. Moutinho, B. To, J. Perkins,
D. Ginley, and H.M. Branz
National Renewable Energy Laboratory

L.R. Tessler
Instituto de Fisica "Gleb Wataghin" Unicamp

D. Han
University of North Carolina at Chapel Hill

*To be presented at the 2003 Materials Research
Society Spring Meeting
San Francisco, California
April 21–25, 2003*



NREL

National Renewable Energy Laboratory

1617 Cole Boulevard
Golden, Colorado 80401-3393

NREL is a U.S. Department of Energy Laboratory
Operated by Midwest Research Institute • Battelle • Bechtel

Contract No. DE-AC36-99-GO10337

NOTICE

The submitted manuscript has been offered by an employee of the Midwest Research Institute (MRI), a contractor of the US Government under Contract No. DE-AC36-99GO10337. Accordingly, the US Government and MRI retain a nonexclusive royalty-free license to publish or reproduce the published form of this contribution, or allow others to do so, for US Government purposes.

This report was prepared as an account of work sponsored by an agency of the United States government. Neither the United States government nor any agency thereof, nor any of their employees, makes any warranty, express or implied, or assumes any legal liability or responsibility for the accuracy, completeness, or usefulness of any information, apparatus, product, or process disclosed, or represents that its use would not infringe privately owned rights. Reference herein to any specific commercial product, process, or service by trade name, trademark, manufacturer, or otherwise does not necessarily constitute or imply its endorsement, recommendation, or favoring by the United States government or any agency thereof. The views and opinions of authors expressed herein do not necessarily state or reflect those of the United States government or any agency thereof.

Available electronically at <http://www.osti.gov/bridge>

Available for a processing fee to U.S. Department of Energy
and its contractors, in paper, from:

U.S. Department of Energy
Office of Scientific and Technical Information
P.O. Box 62
Oak Ridge, TN 37831-0062
phone: 865.576.8401
fax: 865.576.5728
email: reports@adonis.osti.gov

Available for sale to the public, in paper, from:

U.S. Department of Commerce
National Technical Information Service
5285 Port Royal Road
Springfield, VA 22161
phone: 800.553.6847
fax: 703.605.6900
email: orders@ntis.fedworld.gov
online ordering: <http://www.ntis.gov/ordering.htm>



Printed on paper containing at least 50% wastepaper, including 20% postconsumer waste

Combinatorial approach to thin-film silicon materials and devices

Qi Wang, Leandro R. Tessler¹, Helio Moutinho, Bobby To, John Perkins, Daxing Han², Dave Ginley, and Howard M. Branz

National Renewable Energy Laboratory (NREL), 1617 Cole Blvd., Golden, CO 80401 U.S.A.

¹Instituto de Física “Gleb Wataghin,” Unicamp, C. P. 6165, 13083-970 Campinas, SP, Brazil

²Department of Physics & Astronomy, University of North Carolina at Chapel Hill, Chapel Hill, NC, 27599 U.S.A.

Abstract

We apply combinatorial approaches to thin-film Si materials and device research. Our hot-wire chemical vapor deposition chamber is fitted with substrate xyz translation, a motorized shutter, and interchangeable shadow masks to implement various combinatorial methods. For example, we have explored, in detail, the transition region through which thin Si changes from amorphous to microcrystalline silicon. This transition is very sensitive to deposition parameters such as hydrogen-to-silane dilution of the source gas, chamber pressure, and substrate temperature. A material library, on just a few substrates, led to a three-dimensional map of the transition as it occurs in our deposition system. This map guides our scientific studies and enables us to use several distinct transition materials in our solar-cell optimization research. We also grew thickness-graded wedge samples spanning the amorphous-to-microcrystalline Si transition. These single stripes map the temporal change of the thin silicon phase onto a single spatial dimension. Therefore, the structural, optical, and electrical properties can easily be studied through the phase transition. We have examined the nature of the phase change on the wedges with Raman spectroscopy, atomic force microscopy, extended x-ray absorption fine structure (EXAFS), x-ray absorption near-edge spectroscopy (XANES), ultraviolet reflectivity, and other techniques. Combinatorial techniques also accelerate our device research. In solar cells, for example, the combinatorial approach has significantly accelerated the optimization process of p-, i-, n-, and buffer layers through wide exploration of the complex space of growth parameters and layer thicknesses. Again, only a few deposition runs are needed. It has also been useful to correlate the materials properties of single layers in a device to their performance in the device. We achieve this by depositing layers that extend beyond the device dimensions to permit independent characterization of the layers. Not only has the combinatorial approach greatly increased the rate of materials and device experimentation in our laboratory, it has also been a powerful tool leading to a better understanding of structure-property relationships in thin-film Si.

Introduction

The combinatorial approach (high-throughput experimentation) has been applied with success in recent years to thin-film materials research [1-4]. However, the initial work on this approach was begun by Joseph Hanak almost 30 years ago [5]. Hanak made a continuously varied composition sample to study binary composition alloys. As now implemented, the method dramatically shortens the processing time compared to the conventional approach.

Development of computer-automated, high-throughput characterizations makes possible full use of the combinatorial approach. Combinatorial sample deposition, measurements, and data analysis must all be optimized for successful research. Only recently has the combination of deposition tools, computing power, automation, and, more importantly, characterization techniques, become available to allow true combinatorial approaches. In our laboratory, research that previously required up to a year can now be completed in a few weeks.

In spite of more than 25 years of hydrogenated amorphous silicon (a-Si:H) research, the properties of thin-film materials and performance of devices for photovoltaic and related applications remain a significant technical challenge. For example, the properties of undoped thin-film Si that grows near the transition from amorphous to microcrystalline silicon [6, 7] not only depends on the atomic H content in the Si film, but also on many other deposition parameters such as substrate temperature, gas mixture, and gas pressure. Clear fundamental understanding of these better materials is still not established; however, the applications have advanced rapidly. The gradual nature of structural transition and the dependence on multiple deposition variables make the research more difficult. For example, most doped a-Si:H thin films have either B or P doped into a binary alloy (Si and H) or B doped into a tertiary alloy (Si, C, and H). The challenges are even greater because, in applications, the doped a-Si:H materials are normally very thin (tens of nm). In device applications, state-of-the-art solar cells also utilize materials that are grown very close to a structural phase transition to improve performance [7]. In addition to these materials issues, the production of optimized devices is still laboratory dependent: certain procedures are more successful in one lab than others. Each laboratory must perform its own painstaking optimizations on its own deposition equipment. The properties of the materials and the device performance are still lacking strong causal correlations to guide this process to completion. Although there are some general guiding principles, device making is still more often art than science—device optimization has often required years of slow, empirical experimentation. Therefore, amorphous Si and related materials, and the devices made from them, are excellent candidates for using the combinatorial approach. In this paper, we will present our work on amorphous Si based materials and device research using our unique combinatorial hot-wire chemical vapor deposition (HWCVD) system. However, applications of this approach should not be limited to HWCVD. Combinatorial approaches to materials and device research can be used profitably in plasma-enhanced CVD, sputtering, and other deposition techniques.

Combinatorial HWCVD system

In NREL's conventional HWCVD deposition system, a stainless-steel vacuum chamber with a base pressure of less than 10^{-6} Torr is used. A spiral 0.5-mm-diameter, 13-cm-long tungsten wire is heated to about 2000°C using an ac or dc current. The hot wire is normally placed 5 cm below a typically 2.5-cm x 2.5-cm or 6.35-cm x 6.35-cm heated Corning 1737 substrate. Process gases such as SiH_4 decompose on the wire surface. Atomic Si, H, and silane radicals react in the chamber, and reactive radicals form a film on a substrate. For a-Si:H deposition with SiH_4 flow rate of 20 sccm and a chamber pressure of 10 mTorr, a film of device-quality a-Si:H can be deposited at a deposition rate of about 10 Å/s [8].

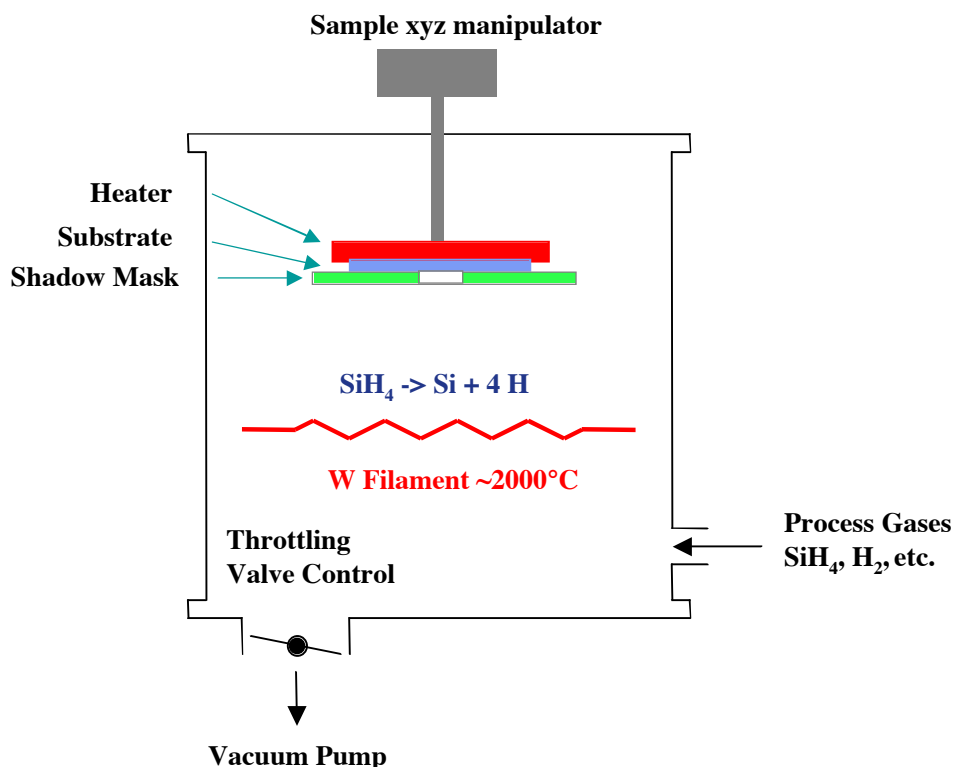


Figure 1. Schematic diagram of the NREL combinatorial HWCVD system.

Figure 1 is a schematic of our combinatorial HWCVD system [9] which is a modified version of NREL's conventional HWCVD system. There are two key modifications: The first is to add a physical mask or a set of masks to deposit the film only on the selected partial area of a substrate. The second is to add a sample manipulator (xyz) that allows a relative xy movement between the mask and the substrate so that the film can be deposited at any position on the substrate. The z-translations are used primarily to move the sample and then ensure a tight contact between the substrate and the mask. This prevents the deposition of materials “shadows” from reactant that would diffuse under loose-fitting masks. The vacuum chamber, filament, and gas inlet are identical to NREL's conventional system. The combinatorial deposition speeds up the sample deposition primarily because pump down cycles between samples are avoided. The system also adds considerable functionality, especially because we have developed a set of masks that are interchangeable in vacuum.

Figure 2 shows the simple example of making a library of discrete variable samples by combinatorial deposition. On the left is a shadow mask with a small open square in the middle. We move the substrate or the mask, using the xy manipulator, to position 1 on the substrate, as indicated in the center figure and deposit the first film. Then, we move the open square to the position 2 and make the second film. The mask isolates each sample from the others. This procedure was repeated for all 16 locations in this example. The optical image shows an actual combinatorial sample on 2.5-cm x 2.5-cm glass substrate. The various gray scales or different colors indicate the thickness or the optical index changes to the various deposition parameters. This approach greatly reduces the time spent on the cycle of loading, heating, and

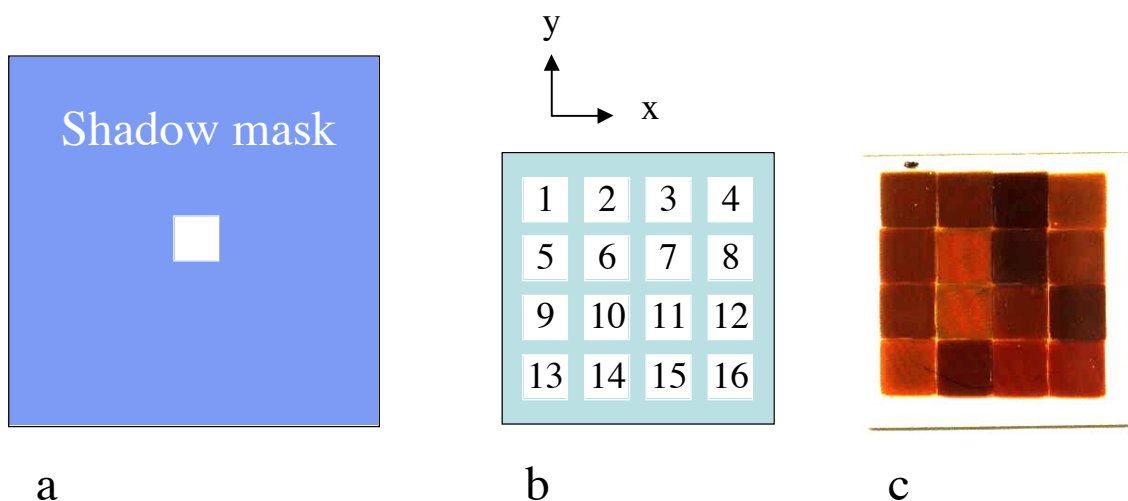


Figure 2. a) Schematic diagram of the mask used to deposit discrete square samples; b) schematic of the sample pattern obtained by stepping the sample beneath the mask between each of 16 depositions; and c) an optical image of the resulting film.

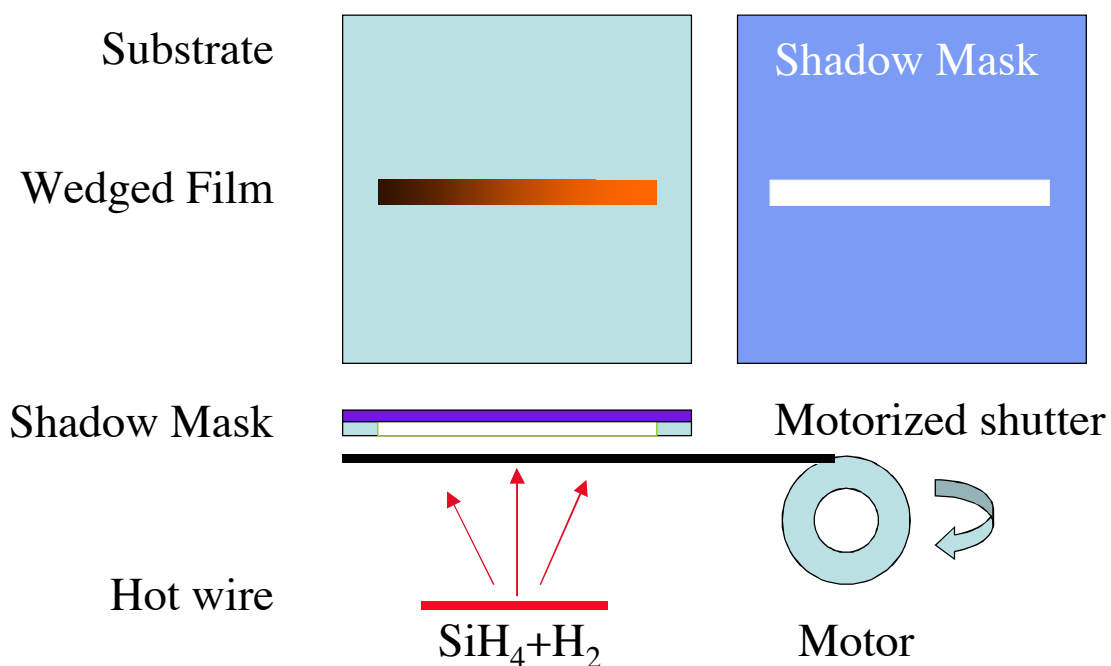


Figure 3. Schematic diagram of the process for making continuously wedged samples with continuously variable thickness. The shutter is placed close to the shadow mask. The motor speed and deposition rate determine the thickness grading.

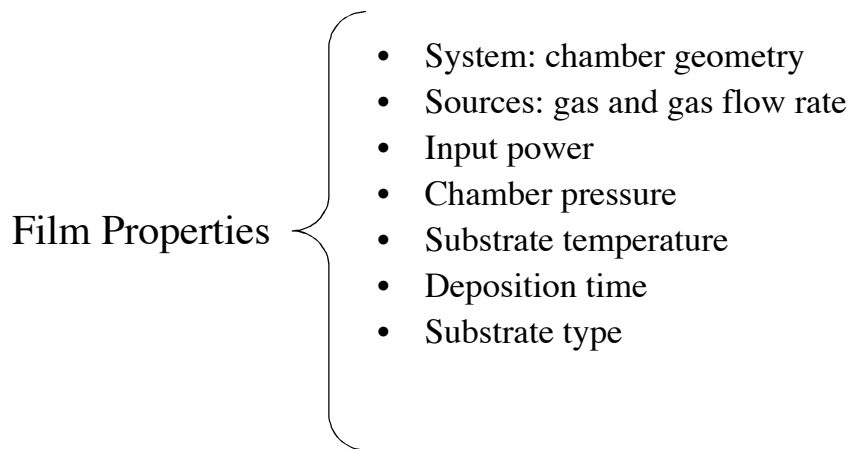


Figure 4. Some deposition factors directly or indirectly determine the thin film properties. This illustration shows the scope of deposition parameters that can be chosen in the combinatorial depositions.

cooling in between the samples in the conventional deposition. A factor-of-10 reduction of total deposition time can be achieved easily.

Figure 3 shows how we make samples with a continuously changing variable such as thickness. In principle, the substrate temperature (by means of the hot and cold ends) and the gas composition (by the means of timing the gas flow rate) can also be continuously changed. To make a thickness-graded stripe sample, a physical mask with a rectangular aperture of 5 x 50 mm and a motor-driven shutter are used. The thickness profile along the stripe is controlled by the motor speed and deposition rate. After the film of one stripe is deposited, the substrate can be moved to another location for deposition of another stripe. Libraries with as many as ten separate wedged stripes are made on a 6.35-cm x 6.35-cm substrate. This combination of discrete and continuous deposition provides a powerful tool to study the sensitive phase transition with regard to the various deposition parameters. We will show our work on the thickness-dependent phase transition from amorphous to microcrystalline silicon on one single substrate below.

In the hot-wire CVD process, many variables, also called “factors,” can affect the amount of SiH_4 in the reaction region, the density of reactants at the film surface and the film formation reactions. These factors, taken together, determine the structure and properties of the films. For a given deposition system, chamber geometry, chamber pressure, source of gas, gas flow rate, direction of gas flow, gas mixture ratio, T_{sub} , substrate, deposition time, filament temperature, distance from filament to the substrate, number of filaments, and post treatments are all important factors. Figure 4 lists some of the important factors in any thin-film deposition that affect the properties of the films. From an engineering point of view, the combinatorial approach dramatically increases the throughput of experimentation and is an ideal tool to map the film properties as a function of many variables. The mapping can be done with a short time even if all the detailed mechanisms of growth are still unknown.

In one study, we selected three variables in the HWCVD process to create a small film library to study the phase transition from amorphous to microcrystalline silicon. Silane flow rate and hydrogen flow rate were obvious and convenient choices. We select the throttling valve position (TVP) as the third variable because it is an independent deposition factor with

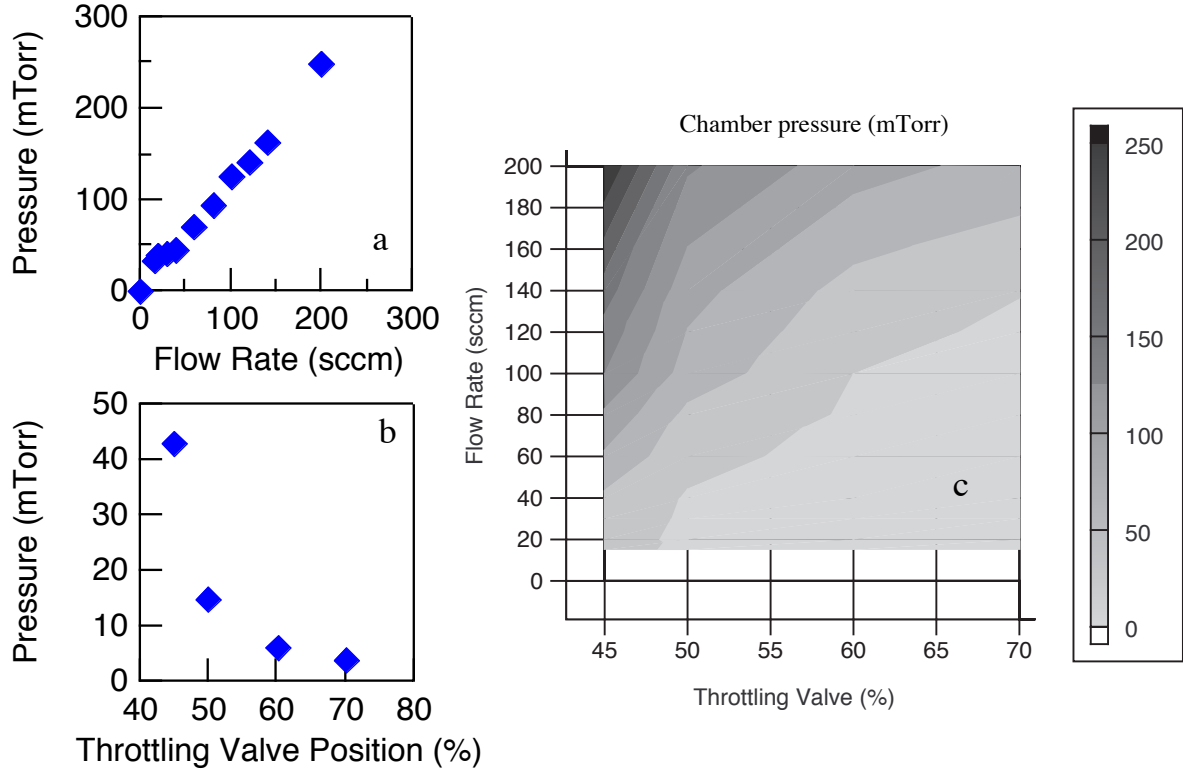


Figure 5. Chamber pressure dependence on the H_2 gas flow rate (a), throttling valve position (b), and in a 2-D contour plot (c). The gray scale on the right indicates the chamber pressure in mTorr.

which we partially control the chamber pressure. We use hydrogen as an example because of its high flow rate. It will apply to other gases, too. The chamber pressure of hydrogen in the chamber depends on the gas flow rate and the TVP. Figure 5 shows how pressure changes with gas flow rate at the fixed TVP of 45 % (Fig. 5a) and with pressure varying with TVP at a fixed gas flow rate of 15 sccm (Fig. 5b). Fig. 5c, shows a contour plot of chamber pressure as a function of a gas flow rate and TVP. To clarify the meaning of TVP, the valve is fully open at 100% and closed at 0%. Pressure has a linear dependence on the gas flow rate (for a fixed TVP of 45%) and rapidly increases with decreasing TVP below 50% (for a fixed gas flow rate of 15 sccm). Due to the nature of the pressure's dual dependence, one can achieve the same pressure by changing the gas flow rate or the TVP. However, the gas pressure alone is not enough to determine that the same material will always be produced. For example, for a-Si:H films with SiH_4 gas, different combinations of gas flow rate and TVP with the same pressure give different films. This is even more complex when using a mixture of gases such as SiH_4 , H_2 , and others. In this paper, we plot our results based on the factor, TVP, even though pressure has a more obvious physical meaning.

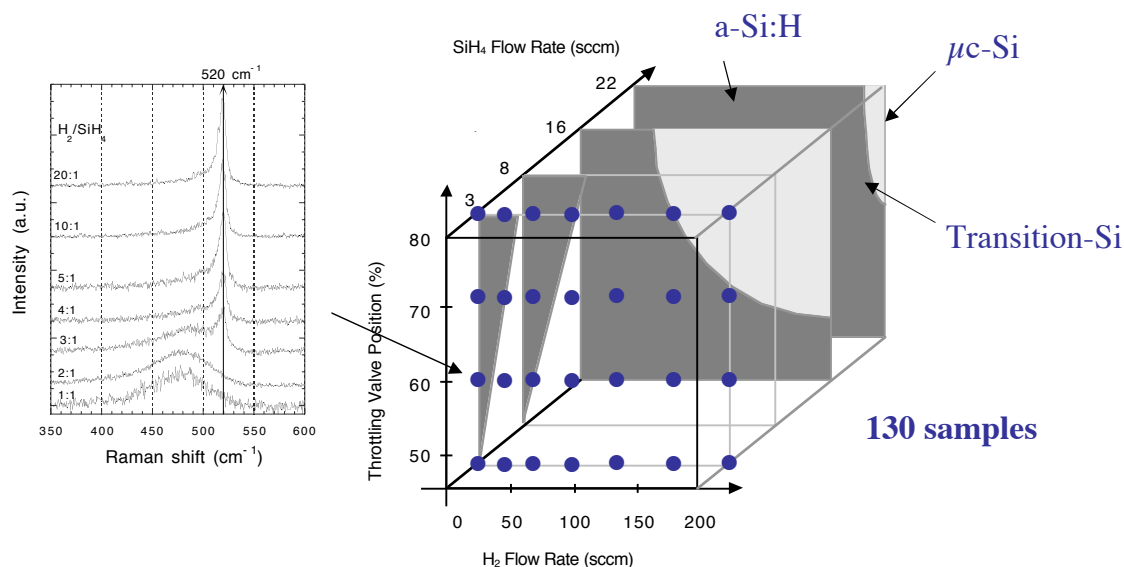


Figure 6. Left, Raman spectroscopy vs. H dilution at TVP of 60% and 3 sccm of silane flow rate. Right, amorphous-to-microcrystalline Si phase diagram as a function of SiH₄ flow rate, H₂ flow rate, and throttling valve positions. The dots represent some of the experimental points where the sample was made. The shaded area denotes a-Si, unshaded is area μc-Si, and the boundary in between is the transition region.

Results and discussion

In this section, we examine several specific examples that demonstrate the power of the combinatorial approach in thin-film Si research. These are (1) a small-scale materials library, (2) a study of the thickness-dependent structure changes, and (3) the effect on a buffer layer at the solar cell p/i interface.

1. Amorphous-to-microcrystalline silicon library

Figure 6 presents the a-Si-to-μc-Si phase diagram as a function of three variables: silane flow rate, hydrogen flow rate, and throttling valve position (TVP, see above). The dots in the figure illustrate the location of the samples in the hydrogen-TVP plane for one of the four silane flow-rates we explored. In total, 130 samples were made sequentially on only 10 substrates (each substrate has less than 16 samples) for a total of 9 vacuum breaks. In each hydrogen-TPV plane, the shaded area represents materials in the amorphous phase and the unshaded area represents material with a microcrystalline phase. The four planes represent silane flow rates of 3, 8, 16, and 22 sccm, respectively. The boundary between the amorphous and microcrystalline phase is where the materials in transition are located. The structure of each sample was determined by the Raman spectroscopy and UV reflectance measurements (Model 1280, n&k Technology, Inc, Santa Clara, CA). Raman spectra at the left of the figure represent a series of H-dilution samples with silane flow rate of 3 sccm and TVP at 60%.

We found that the material phase depends nonlinearly on all the variables: hydrogen flow rate, silane flow rate, and the throttling valve position. From Fig. 6, one sees that the ratio of hydrogen to silane is not a unique factor that describes whether the material will grow amorphous or microcrystalline. At the lowest silane flow rates (3 and 8 sccm), it is easy to change to $\mu\text{c-Si}$ with the mixture of only a small amount of H_2 . At higher silane flow rates (16 and 22 sccm), it requires higher H dilutions and an open throttle valve to deposit $\mu\text{c-Si}$. This film library has guided us for our many HW solar cells applications. Note that this phase diagram is based entirely on measurement of thick (>200 nm) films. The thickness dependence of the phase transition was addressed in a study of continuously thickness-graded samples as described below.

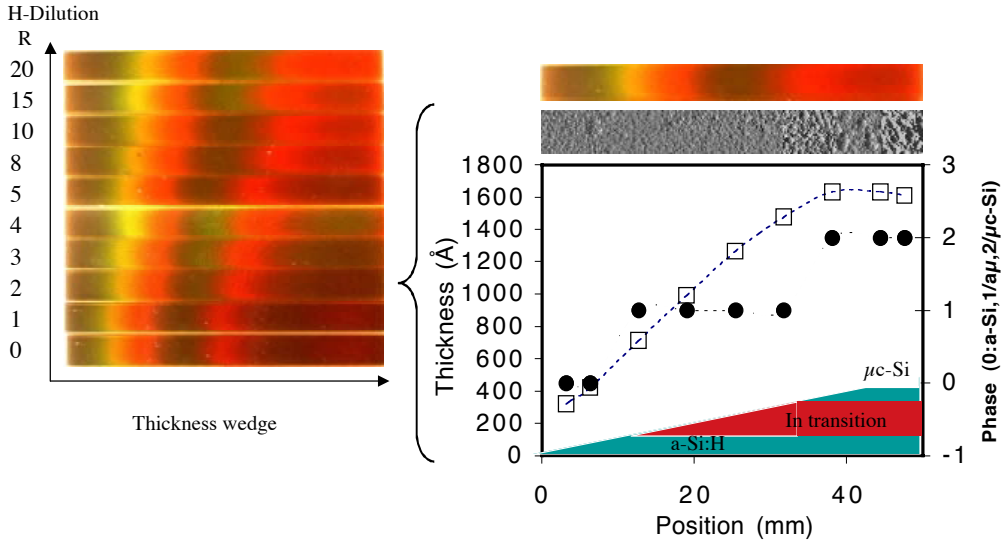


Figure 7. Thickness dependence of a-Si-to- $\mu\text{c-Si}$ phase transition in samples continuously graded thickness. Left, an optical image of a combinatorial sample with a thickness grading in horizontal direction and H-dilution in the vertical direction, as indicated by the R for each stripe. Right, a summary plot on the stripe number 2 of $R = 2$. The optical image of the stripe is placed on the top, and a collections of six AFM pictures with roughly matched positions on the stripe is under that. The figure below shows the thickness variation and the phase changes along the stripe. The insert cartoon best describes the profile of the interesting stripe with a large portion of transition materials.

2. Thickness-dependent phase transition

The left picture in Fig. 7 is an optical-reflection image obtained by placing a ten-stripe continuously thickness-graded sample in a conventional color image scanner. This sample has discrete H-dilution stripes arrayed in the vertical direction, deposited with H_2 -to- SiH_4 ratios (R) of 0, 1, 2, 3, 4, 5, 8, 10, 15, and 20. The SiH_4 flow rate was fixed at 8 sccm. Each stripe has a thickness grading ranging from about 200 to 1600 Å. This special sample varies by two deposition parameters: ten discrete H-dilutions and continuously varied thicknesses. From these

parameters, we can construct an evolutionary-phase diagram as a function of H-dilution and thickness for HWCVD Si by measuring the Raman or UV reflectance of the sample [10, 11]. The substrate temperature is 200°C, and the chamber pressure ranges from 6 to 57 mTorr, depending on R. The total deposition time for the entire 10-stripe sample was just over 2 hours. The gray scale change along each stripe indicates the thickness variation. The gray scale or color shift among the stripes directly indicates both the decrease of deposition rate and an increase of $\mu\text{c-Si}$ fraction in the film with increasing R.

By measuring UV reflectance and observing the peaks at 275 and 360 nm, we are able to quickly determine whether or not there is crystallinity within the top 100 Å of the film [3, 12]. We found that with $R > 2$, all the stripes are in $\mu\text{c-Si}$ phase everywhere on the stripes. The stripe with $R=0$, as expected, is entirely the a-Si phase. The stripe with $R=1$ was amorphous along most of its length, showing the signal of $\mu\text{c-Si}$ only at the thickest end. The stripe with $R=2$ has a long transition phase. For this reason, it is of the greatest interest, and we have simulated it accordingly to the need to develop high-throughput characterization techniques to measure this special stripe.

The right side graph in Fig. 7 is a summary plot of film properties of surface morphology, thickness, and corresponding phase along the stripe. The top picture is a scanner image of the stripe. Just below this image is a composite of six AFM images arranged to be in roughly the correct position on the stripe. This composite AFM image shows that the a-Si:H surface is rather smooth compared to the much rougher $\mu\text{c-Si}$. Interestingly, a large range in the middle of the stripe appears rather smooth, although the UV reflectivity and Raman measurements revealed that this material is already undergoing the phase transition at this thickness. The roughness is about 10 Å for a-Si:H, 15 Å for transition materials, and 46 Å in the $\mu\text{c-Si}$. The thickness of this stripe changes from 200 to 1600 Å across its 50-mm length, as shown in the main graph. The thickness increases quite linearly from 200 to 1600 Å along the positions from 0 to 40 mm. However, in the last 10 mm the thickness is quite constant because (1) the deposition rate decreases when $\mu\text{c-Si}$ growth commences and (2) there is some deposition rate inhomogeneity in our HWCVD reactor. To plot phase results, we denote a-Si:H with a 0; transition or mixed phase Si as 1; and $\mu\text{c-Si}$ as 2. For thicknesses less than 600 Å, the material is in a-Si:H phase. For thicknesses of more than 1500 Å, $\mu\text{c-Si}$ starts to grow, and between 600 and 1500 Å, the material appears to be mixed phase (in transition). The wedge cartoon is a schematic illustration of the phase evolution from amorphous-to-microcrystalline silicon in this stripe. Our results are in qualitative agreement with Collins' in-situ ellipsometry measurement for PECVD films [13].

Figure 8 shows the extended x-ray absorption fine structure (EXAFS) (Fig. 8a) and which x-ray absorption near-edge spectroscopy (XANES) (Fig. 8b) results on the stripe (Fig. 7) that has a large section of transition region from the amorphous-to-microcrystalline phase. The EXAFS spectra have been measured along the stripe from a-Si:H to $\mu\text{c-Si}$ as indicated with sample coordinate x. From EXAFS spectra, one can perform numerical fitting to get the average interatomic distance (r) and the radial Debye-Waller factor (σ_{incr}^2). The detailed fitting procedure has been published elsewhere [14]. The results in Fig. 8a show the decrease of σ_{incr}^2 (which becomes negative) and the subtle decrease of r as the crystalline fraction of the sample increases. The negative σ_{incr}^2 is a consequence of the imposed average coordination $N = 4$: the average coordination of both a-Si:H and $\mu\text{c-Si}$ are expected to be below 4, and imposing a higher coordination is compensated by a decrease in σ_{incr}^2 .

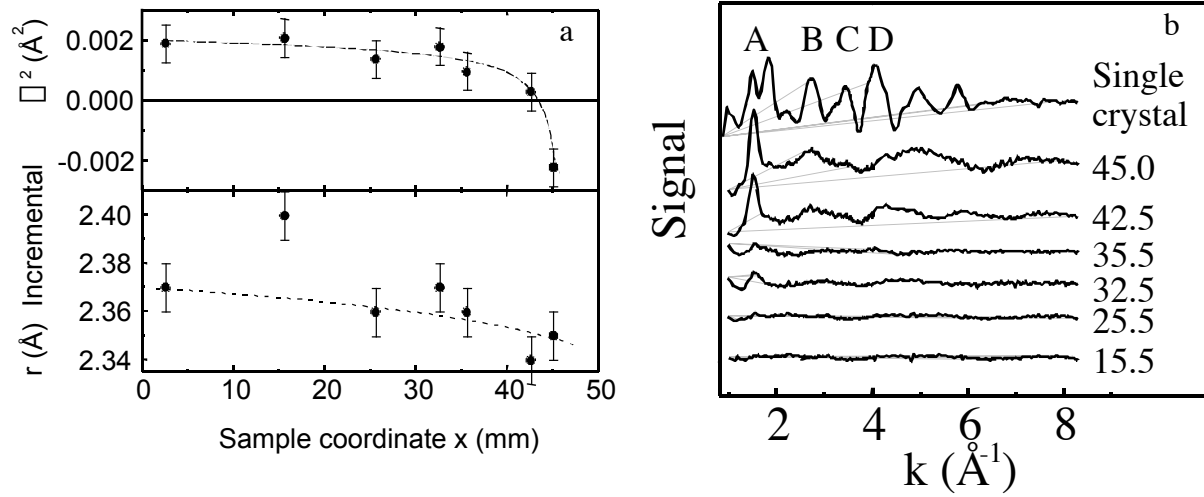


Figure 8. EXAFS study (Fig. 8a) and XANS study (Fig. 8b) on the strips sample in Fig. 7.a), incremental Debye-Waller factor (relative to single-crystal Si), and average first neighbor separation. Four fold coordination was imposed in the fitting procedure. The lines are guides for the eye. (b) x-ray absorption spectroscopy signal with the single scattering (EXAFS) contribution subtracted. The numbers in the figure represent the x coordinate, and the letters follow the peak assignment. The coordination is the same as in Fig.7.

Figure 8b show the XANS spectra at various positions on the stripe together with that of a c-Si reference [15]. In the single crystal, we can clearly identify the A, B, C, and D multiple scattering peaks that are attributed to double scattering paths. In the a-Si:H side of the sample, no peaks are found. In the μ c-Si side, only peak A can be identified. In order to isolate the multiple scattering effects, we have subtracted all spectra from the one obtained at $x = 2.5$ mm, where only a-Si:H is present. In the a-Si part of the sample, indeed, there are no multiple scattering signals. In the μ c-Si part, the dominating path is due to scattering by two adjacent atoms of the first coordination shell. This surprising result indicates that the bond-angle disorder of μ c-Si is enough to suppress the multiple scattering signals from atoms beyond the first coordination shell. In amorphous silicon, bond-angle disorder suppresses even the contribution from the first shell. The main consequence of this result is that the μ c-Si formed at the transition region and even at the end of the strip (highly μ c-Si) is much more disordered than single crystal-silicon —to a point that the second-neighbor shell disorder is comparable to the first-neighbor shell disorder in a-Si:H.

3. Optimization of devices

In the thin-film devices such as solar cells, the device structure combines three or more layers. This structure is naturally suited for the combinatorial HWCVD approach because different masks can be used on each layer, thereby giving more information than in conventional devices. Certainly, all device-makers would like to know how the properties of each layer relate to device performance. By using the combinatorial approach, this kind of insight can be obtained.

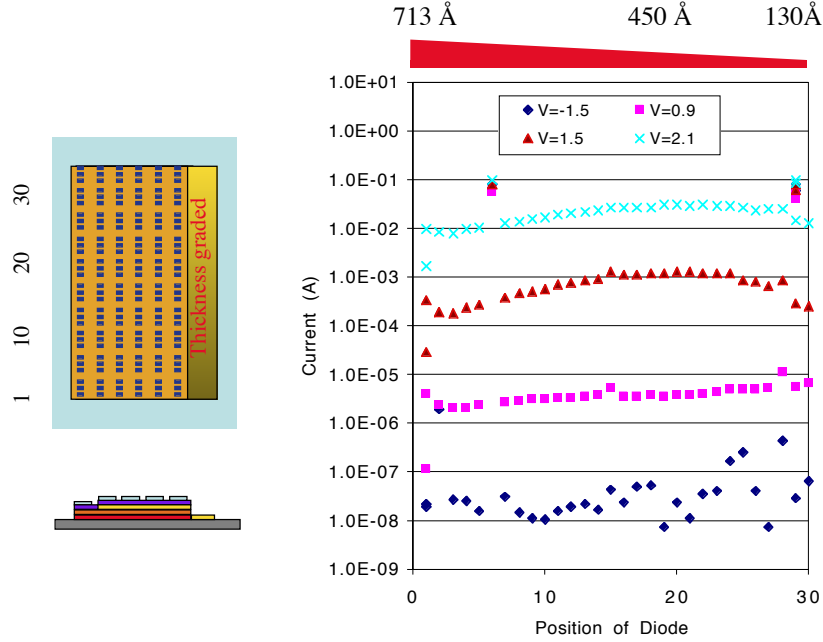


Figure 9. Effects of a buffer layer and its thickness at p/i interface on a diode in one combinatorial sample. Left, a schematic of device n-i-b-p structure and layer locations (top and side views) of the combinatorial sample. The top dot array is the top contact to evaluate the devices. The thickness-graded buffer layer is deposited at the p/i interface, but offset to have the buffer layer on the substrate. Right, the dark current as a function of the positions (the buffer layer thickness) at various voltage biases. The scale of the thickness is plotted on top of the figure.

Figure 9 shows a combinatorial device we made to study the effect of a single device layer—the thin buffer (b) layer between the p and i-layers—on diode performance. A schematic of the device structure is shown on the left. Using a single mask, the thickness graded buffer layer was offset from the n-i-p diode. In this way, part of the buffer layer was incorporated into the device and part was deposited directly on the substrate. The cross section of the device shows that n-i-p, n-i-b-p, and b can be measured independently. In the perpendicular direction, the thickness of the buffer layer was graded. The 50-mm-long wedge incorporates 30 top Pd contacts that we used to evaluate the device performance versus thickness. The thickness of the buffer layer was directly measured on the offset b-layer. The graph shows the logarithm of the dark current at various voltage biases, plotted as a function of diode position. The diode position is directly related to the thickness of the buffer layer, as indicated schematically by the triangular wedge above the graph. The results show that the buffer layer has little effect on the reverse current but does affect the forward current. At V=1.5 V and with 450 Å of buffer layer the dark current, increases by about a factor of 10 when compared to either the zero- or 700-Å-thick buffer layers. With only one sample, the effect of buffer layer and its thickness on the device performance can be readily studied.

Summary

We have demonstrated that combinatorial studies can be a powerful tool for materials and device research in thin-film silicon. The combinatorial samples have not only greatly speeded up the deposition process, but also stimulated development of many high-throughput characterizations to measure the samples. Developing fast characterization and data analysis tools for a large number of samples has become critical for optimizing processes and searching for new materials. With our combinatorial HWCVD tool, we efficiently created a material library of the transition from a-Si:H to μ c-Si and were able to use this information to guide our device research. We were able to provide new XANES information about the transition material and hope to accelerate the understanding of ordering in the transition materials. For thin-film device applications, we demonstrated that the combinatorial approach can also make important contributions to device optimization and to correlation of films properties to device performance. Increasing the experimental efficiency, i.e., the experimental throughput, is a central motivation for the combinatorial approach. Based on our initial work, the combinatorial approach has speeded up the rate of experimentation by at least a factor of 10 in our HWCVD thin-film Si research.

Acknowledgements

The author would like to thank Richard Crandall, Brent P. Nelson, and Yueqin Xu for discussions and help. This work is supported by the U.S. Department of Energy under subcontract No. DE-AC39-98-GO10337 and DDRD research funded at NREL.

REFERENCES

1. X.-D. Xiang, X. Sun, G. Briceno, Y. Lou, K.-A Wang, H. Chang, W. G. Wallace-Freedman, S.-W. Chen, and P.G. Schultz, *Science*, **268**, p. 1738, 1995.
2. X-D. Xiang, *Materials Science & Engineering. B*, **56**, p. 247, 1998.
3. Qi Wang, Guozhen Yue, Jing Li, and D. Han, *Solid State Commun.*, **113** p. 175, 2000.
4. Qi Wang, J. Perkins, H. Branz, J. Alleman, C. Duncan, and D. Ginley, *Applied Surface Science*, **189** p. 271, 2002.
5. J.J. Hanak, *J. Mat. Science*, **5** p. 964, 1970.
6. L. Yang and L.-F. Chen, *Mat. Res. Soc. Proc.*, **336**, p. 669, 1994.
7. J. Yang and S. Guha, *Mat. Res. Soc. Proc.*, **557**, p. 239, 1999.
8. A.H. Mahan, J. Carapella, B.P. Nelson, R.S. Crandall, and I. Balberg, *J. Appl. Phys.*, **69** p. 6728, 1991.
9. Qi Wang, *Thin Solid Films*, (2nd HWCVD Conference) to be published, 2003.
10. G.Z. Yue, J. D. Lorentzen, J. Lin, D.X Han, and Q. Wang, *Appl. Phys. Lett.*, **67** p. 3468, 1999.
11. G.Z. Yue, J. Lin, L. Wu, D.X. Han, and Q. Wang, *Mat. Res. Soc. Proc.*, **557**, p. 525, 1999.
12. D.L. Greenaway, G. Harbeke, *Optical Properties of Semiconductors*, Pergamon, New York, 1968.
13. R. W. Collins, J. Koh, A.S. Ferlauto, P.I. Rovira, Y. Lee, R.J. Koval, and C.R. Wronski. *Thin Solid Films*, 364, p.129. 2000.
14. Leandro R. Tessler, Q. Wang, and H.M. Branz, *Thin Solid Films*, (2nd HWCVD Conference) to be published, 2002.
15. J. J. Rehr, and R.C. Albers, *Rev. Mod. Phys.*, **72** p. 621, 2000.

REPORT DOCUMENTATION PAGE			Form Approved OMB NO. 0704-0188	
Public reporting burden for this collection of information is estimated to average 1 hour per response, including the time for reviewing instructions, searching existing data sources, gathering and maintaining the data needed, and completing and reviewing the collection of information. Send comments regarding this burden estimate or any other aspect of this collection of information, including suggestions for reducing this burden, to Washington Headquarters Services, Directorate for Information Operations and Reports, 1215 Jefferson Davis Highway, Suite 1204, Arlington, VA 22202-4302, and to the Office of Management and Budget, Paperwork Reduction Project (0704-0188), Washington, DC 20503.				
1. AGENCY USE ONLY (Leave blank)		2. REPORT DATE April 2003		3. REPORT TYPE AND DATES COVERED Conference Paper Preprint
4. TITLE AND SUBTITLE Combinatorial Approach to Thin-Film Silicon Materials and Devices: Preprint			5. FUNDING NUMBERS PVP34101	
6. AUTHOR(S) Q. Wang, L.R. Tessler, H. Moutinho, B. To, J. Perkins, D. Han, D. Ginley, and H.M. Branz				
7. PERFORMING ORGANIZATION NAME(S) AND ADDRESS(ES) National Renewable Energy Laboratory, 1617 Cole Blvd., Golden, CO 80401-3393 Instituto de Fisica "Gleb Wataghin," Unicamp, C.P. 6165, 13083-970 Campinas, SP. Brazil Department of Physics & Astronomy, University of North Carolina at Chapel Hill, Chapel Hill, North Carolina 27599			8. PERFORMING ORGANIZATION REPORT NUMBER NREL/CP-520-33070	
9. SPONSORING/MONITORING AGENCY NAME(S) AND ADDRESS(ES)			10. SPONSORING/MONITORING AGENCY REPORT NUMBER	
11. SUPPLEMENTARY NOTES				
12a. DISTRIBUTION/AVAILABILITY STATEMENT National Technical Information Service U.S. Department of Commerce 5285 Port Royal Road Springfield, VA 22161			12b. DISTRIBUTION CODE	
13. ABSTRACT (<i>Maximum 200 words</i>): We apply combinatorial approaches to thin-film Si materials and device research. Our hot-wire chemical vapor deposition chamber is fitted with substrate xyz translation, a motorized shutter, and interchangeable shadow masks to implement various combinatorial methods. For example, we have explored, in detail, the transition region through which thin Si changes from amorphous to microcrystalline silicon. This transition is very sensitive to deposition parameters such as hydrogen-to-silane dilution of the source gas, chamber pressure, and substrate temperature. A material library, on just a few substrates, led to a three-dimensional map of the transition as it occurs in our deposition system. This map guides our scientific studies and enables us to use several distinct transition materials in our solar-cell optimization research. We also grew thickness-graded wedge samples spanning the amorphous-to-microcrystalline Si transition. These single stripes map the temporal change of the thin silicon phase onto a single spatial dimension. Therefore, the structural, optical, and electrical properties can easily be studied through the phase transition. We have examined the nature of the phase change on the wedges with Raman spectroscopy, atomic force microscopy, extended x-ray absorption fine structure (EXAFS), x-ray absorption near-edge spectroscopy (XANES), ultraviolet reflectivity, and other techniques. Combinatorial techniques also accelerate our device research. In solar cells, for example, the combinatorial approach has significantly accelerated the optimization process of p-, i-, n-, and buffer layers through wide exploration of the complex space of growth parameters and layer thicknesses. Again, only a few deposition runs are needed. It has also been useful to correlate the materials properties of single layers in a device to their performance in the device. We achieve this by depositing layers that extend beyond the device dimensions to permit independent characterization of the layers. Not only has the combinatorial approach greatly increased the rate of materials and device experimentation in our laboratory, it has also been a powerful tool leading to a better understanding of structure-property relationships in thin film Si.				
14. SUBJECT TERMS: PV; hot-wire chemical vapor deposition; x-ray absorption near-edge spectroscopy (XANES); extended x-ray absorption fine structure (EXAFS); Raman spectroscopy; atomic force microscopy; microcrystalline silicon;			15. NUMBER OF PAGES	
			16. PRICE CODE	
17. SECURITY CLASSIFICATION OF REPORT Unclassified	18. SECURITY CLASSIFICATION OF THIS PAGE Unclassified	19. SECURITY CLASSIFICATION OF ABSTRACT Unclassified	20. LIMITATION OF ABSTRACT UL	